DOI 10.1007/s11595-017-1572-3

Friction and Wear Behaviors of Ti/Cu/N Coatings on Titanium Alloy Surface by DC Magnetron Sputtering

LI Junxia[1,2,3], PANG Xiaoxu[4], FAN Ailan[3*], ZHANG Huiqiao[3]

(1.College of Mechanical Engineering, Taiyuan University of Technology, Taiyuan 030024, China; 2.Shanxi Provincial Engineering Laboratory (Research Center) for Mine Fluid Control, Taiyuan 030024, China; 3.Research Institute of Surface Engineering, Taiyuan University of Technology, TaiYuan 030024, China; 4.Henan University of Science and Technology, Luoyang 471027,China)

Abstract: Ti/Cu/N coatings with different Cu contents were deposited on titanium alloy surface by the DC magnetron sputtering technique. XPS and FESEM were employed to characterize the composition and structure of the coating on the Ti6Al4V substrates. In addition, The adhesion force, friction, and wear properties of the Ti/Cu/N coatings were investigated. The experimental results showed that the coarse particles of the coatings would grow more and the surface roughness increased with the increase of copper content in the coatings; The coatings showed a strong adhesion force; The friction coefficient of the coating of the samples was less than the substrate, reaching 0.19 at least. The wear resistance of the coatings could be improved by optimizing and controlling the relative content of Ti, Cu, N elements on the titanium alloy surface, especially the 10.98 at% contents of the copper. The sample C2 kept the best wear resistance.

Key words: titanium alloy substrate; DCMS; coating; friction; wear

1 Introduction

Titanium and titanium alloy are widely used in many industrial fields due to their excellent corrosion resistance and mechanical properties[1]. However, the poor tribological behavior of the titanium and titanium alloy limits their wide applications[2]. So the research about the modifying properties of the surface of titanium is still conducted[3].Nowadays,a series of different surface modification techniques, such as physical and chemical vapor deposition(PVD/CVD) [4], thermal oxidation[5], ion implantation[6], plasma spraying[7] and arc reactive ion plating[8]have been developed to improve the tribological properties of the coatings. In addition, a number of titanium alloy-based coatings are deposited by applying different techniques, such as multicomponent (TiAlCN,TiNOC) [9,10], multilayer (TiN/TiCN/TiC)[11] and graded (Ti/TiN/TiCN)[12]. In fact, although more surface modification techniques have been proposed and considerable progress has also been achieved for the latest decades, each technique and coating have their own advantages and disadvantages. For PVD/CVD, thermal oxidation, ion implantion, the high temperatures destroy the physical properties of the coating[13]. For multilayer (TiN/TiCN/TiC), although the thickness is enough, and it prolongs the service life of the coating, tribological behaviors indicate that there is no significant change in the wear resistance of the coating as compared with those of other thin hard coatings [14].

C and Cu are both good solid lubrication materials, but the hardness of the coatings contained Cu element is investigated only. The effects of Cu on the composition, structure, and hardness of these nanocomposite Ti/Cu/N films deposited by pulse biased arc ion plating were investigated[15-17,18]. It was showed that Ti/Cu/N coatings containing 1.5 at% of copper exhibited maximum hardness of 45 GPa and relatively low friction coefficient of 0.3. The Ti/Cu/N coatings showed a better wear resistance than the 316L SS substrate due to the high surface hardness of intermetallic precipitation of TiN by plasma surface alloying technique[19].

This study presents Ti/Cu/N coatings on titanium alloy surface by direct current magnetron sputtering(DCMS) technique, which has low preparing temperature and good adhesion force between the coating and the substrate [20-22]. The microstructure, mechanical properties and friction and wear behaviors of the Ti/Cu/N coatings were investigated.

(Received: Dec. 29, 2015; Accepted: Nov. 16, 2016)

LI Junxia(李军霞): Prof.; Ph D.; E-mail: bstljx@163.com

*Corresponding author: FAN Ailan(范爱兰): Assoc. Prof.; Ph D; E-mail: ailanfan@163.com

Funded by the Science and Technology Project of Shanxi Province (No.2015031006-2), the NSFC- Shanxi Coal Based Low Carbon Joint Fund Focused on Supporting Project (No.U1510205) and the New Century Excellent Talents(No.NECT-12-1038)

2 Experimental

2.1 Specimens preparation

Ti6Al4V wafers with the size of ϕ10 mm×3 mm were used as the substrates. The Ti/Cu/N coatings were obtained by using DCMS system (Beiking Chuangshi Weina Technology Co., Ltd, JS2S-100B). After ground with No.360-2000 emery papers, the substrates were polished with the diamond polishing agent spray. Before putted into the sputtering chamber, all of the substrates were ultrasonically cleaned for 10 min in acetone and ethanol respectively. Then the substrates were rinsed and dried with deionized water. The titanium targets (99.99% purity) were inlaid with copper (99.99% purity), embedded in the etching area by DCMS. The diameters of the three copper bars were ϕ1 mm, ϕ3 mm, ϕ5 mm, and the relative area ratios of the Cu and Ti target were 0.16%, 1.44% and 4%. The corresponding titanium targets inlaid with copper were marked as C1, C2, C3.

The process parameters were as follows: the Ar/N_2 maxture gas pressure was 0.6 Pa (Ar:N_2=1 :1). The pressure of nitrogen was 0.3 Pa.The source voltage was controlled in a range of 350-380 V, the target current of 0.8-1 A . The distance from the substrate sample to the source target was 80 mm. In order to improve the substrate temperature and increase adhesion force, the deposition was conducted at a bias voltage of 80 V. The process duration was 2 h.There were two steps in the experiment :(1) At the first hour, the argon was only pumped into the vacuum chamber, the sputtering pressure was 0.6 Pa, the firstly deposited Ti/Cu coating could be beneficial to good adhesion force[23]. (2) At the second hour, the mixed gas of the equivalent N_2 and Ar was pumped in and the nitrogen was selected as the reactive gas, while the argon was selected as the working gas. Then keeping the sputtering pressure unchanged, the Ti/Cu/N coatings were obtained.

2.2 Structural characterizations

Microstructural analysis was performed on the surface of the Ti/Cu/N coatings by Nano SEM430. The chemical state of the coatings was determined by VG ESCALAB Mark II X-ray photoelectron spectroscopy (XPS) with Al Kα false X-ray as the radiation source.

2.3 Mechanical characterization and tribological test

The adhesion strength of the coatings to the substrate was measured using a HT-3002 Micro Scratch Tester (Zhejiang Huijinteer Coating Technology co., LTD), which has a conical diamond tip of 0.2 mm radius and 120° taper angle. And the starting and max load was 5 and 30 N respectively.The scratching speed was 2 mm/min, and the loading speed was 20 N/min. The morphology of the scratch was detected by optical microscopic examination (Zeiss Axiovert 25CA).

Drying sliding friction and wear tests were carried out using the ball-on-disk reciprocating tribometer (MFT-R4000 produced by Lanzhou Institute of Chemical Physics Chinese Academy of Sciences) at room temperature of about 25±3 ℃. An alumina ball of 5 mm in diameter was used as the counter face. During the test, the sample to be tested was rotated against the stationary ball under applied loads of 1 N. The sliding frequency of the sample relative to the ball was 2 Hz, the sliding distance was 5 mm, and the testing time was 1 500 s. The coefficient of friction was recorded continuously during the test by a computer data-requisition system.

3 Results and discussion

3.1 Microstructure

In the experiment, XPS was used to determine the composition of the Ti/Cu/N coatings. The contents of copper are listed in Table 1.

Table 1 The rates of copper in the coatings

Sample	C1	C2	C3
Cu/at%	0.81	10.98	19.89

The SEM morphologies of different samples are shown in Fig.1.The surface of the sample C1 coating is smooth, as shown in Fig.1(a). The surface of sample C3 shows the granular structure, which is similar to the

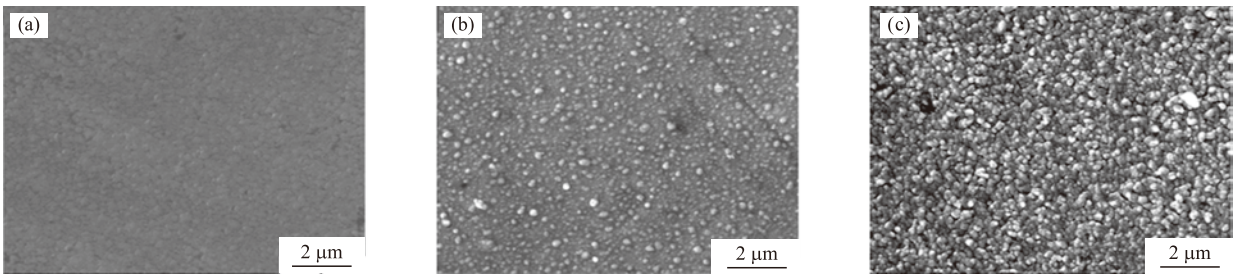

Fig.1 SEM images of Ti/Cu/N coatings deposited with different copper content targets: (a) C1; (b) C2; (c) C3

result of the Thornton model[24]. It could be concluded from Fig. 1 that the coatings were dense with a distinct granular structure and grain boundary, so it was called "large particles". With an increase of the Cu contents in the coatings, the number of large particles increases. Therefore, the surface roughness of the samples increased with the increase of the Cu contents in the titanium target.

The glow-discharge optical omission spectrometry (GD-OES) was employed to confirm the variation of the composition for the three samples coatings. Fig.2 shows the GD-OES spectra of the concentration distribution along the coating depth.The thickness of the coating could be seen from the Cu concentration, about 4-9 μm.The coating was divided into two layers obviously: the uppermost Ti/Cu/N layer and the Ti/Cu layer close to the substrate. Fig.2 gives the distribution curves of the samples C1, C2, C3.The thickness of the Ti/Cu/N layer is 0.5 μm, and the Ti/Cu layer is about 4 μm, as could be seen from Fig.2(a).The Ti concentration sharply rises from 55 wt% to 97 wt% at the distance of 0-0.5 μm, and then keeps the value to the 3 μm depth of the coating, at last the value slightly reduces to 95 wt%;The Cu concentration is stable and small, about 2 wt%,and when the depth of the coating is about 3.7 μm,the value is zero; The N concentration sharply diseases from 40 wt% to 0 wt% at the 0-0.5 μm depth of the coating, and the change is just the opposite to the Ti concentration.The Al and V elements of the substrate appear at the depth of 3.7 μm.

Fig.2 (b) shows that the content of Ti is around 40 wt% at the begining, and rises rapidly at 1 μm which reaches 84 wt%, then the concentration rises slowly to 90 wt%; The content of Cu on the surface will decrease from 38.4 wt% to 12 wt%,then rises slowly from 14.3 wt% to 20.6 wt%, and decreases at the 6.2 μm which has a contrary changing tendency with Ti element, at the distance of 9 μm,the content of Cu will decrease to 0.3 wt%; The distribution of element N keeps in 22 wt% from surface to 1.5 μm, then falls rapidly to 1.5 wt% in the 1.8 μm, then falls slowly;The Al and V elements of the substrate appear at the depth of 6 μm.

Fig.2(c) shows that the content of Ti increases rapidly from 35 wt% to 78 wt%, it begins to fluctuate at the depth of 3.1 μm, then rises at the 3.4 μm up to 90 wt%; The highest content of Cu is 41 wt%, and decreases at the 0.7 μm which has a contrary changing tendency with Ti;The highest content of N is 43 wt%, then it decreases obviously to 22 wt%; At the depth of 3 μm, the Al and V elements of the substrate appear. In Ti / Cu coating, the GDOES map shows that the changing trends of Ti and Cu thickness are contrary; In Ti / Cu / N coating, the changing thickness of the Ti, Cu and N elements influence each other.

Fig.3 is the EDS energy spectra of the sample film. As can be seen, the film mainly consisted of the Ti, Cu and N, the content of Ti in sample C1 was 59.43%, the content of Cu was 0.81%, and the content of N was 39.76%. In sample C2, the content of Ti was 47.61%, the content of Cu was 10.98%, the content

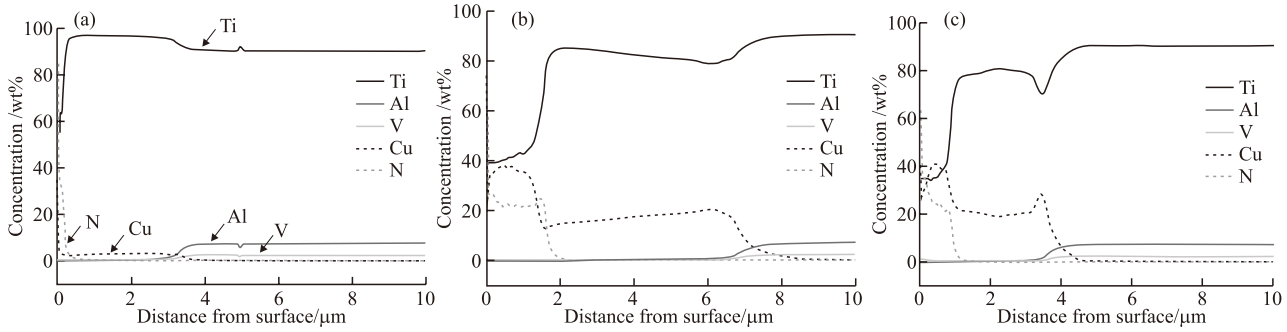

Fig.2 Elements distribution of the films: (a) C1, (b) C2, (c) C3

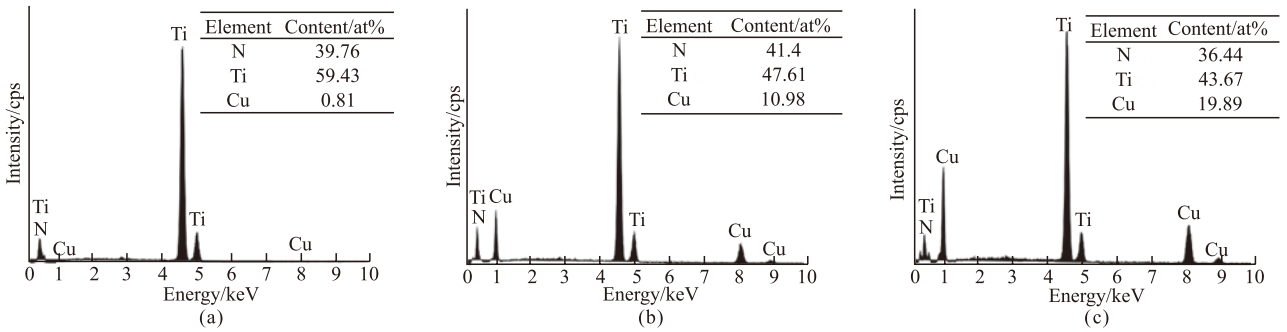

Fig.3 EDS images of the coating: (a) C1; (b) C2; (c)C3

of N was 41.4%. In sample C3, the content of Ti was 43.67%, the content of Cu was 19.89%, the content of N was 36.44%. The result also shows that the content of Cu in the film was related to the target composition, and the content of Cu increased with the increase of the relative area of Cu. In Fig.3, the relative content of the element Cu was up to 19.89%, the lowest content was only 0.81%. It can also be seen that the curve peaks of N element and the Ti element were overlapping which was caused by the production of Ti/N. The analysis result shows that elements of Ti, Cu, N deposited on the substrate successfully.

3.2 Scratch morphology

Fig.4 gives the micrograph of the scratch track of samples C1, C2 and C3. When the conical diamond tip started to slid along the coating surface, a plastic deformation appeared on the coating-substrate system. The scratch became more severe with the increase of the sliding time and load. In addition, a less uplift deformation could be found on the outside of the scratches. When the loads increased to approximate maximum 30 N, the uplift deformations and coating fracture were obvious (Fig.4(a)). The serious uplifting phenomenons could be found in the terminal of the scratch. However, we did not capture the coating and substrate layer in the microscope. From Fig.4 (a), we can also observe that the scratch was smooth.

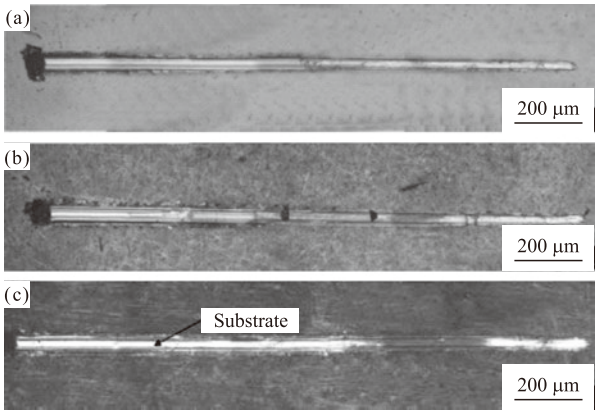

Fig. 4 Morphology of scratch track: (a)C1; (b) C2; (c) C3

We can observe that nick was rough around the scratch from Fig.4 (b). Moreover, the tension cracks were obvious, and even extended to the outside of the scratch. The fracture phenomenon was found around the scratch (Fig.4 (b)), which is likely to be caused by the peeling of the coating. Finally, the continuous peeling of the coating appeared on the left side of the scratch.

Fig.4(c) shows the micrograph of the scratch track of sample C3. The silvery luster and light substrate layer were found in the scratch track .Therefore, it could be concluded that the coating of sample C3 failed, which was caused by flaking.

During the test, the soft coating fails which may be caused by deviating induced by the compressive stress concentration, since the tip had a direct extrusion effect on the front of the tip and resulted in the compressive stress concentration. With the increase of the load, the adhesion force between the coating layer and the substrate layer became strong. However, the coating did not deviate from the substrate. Therefore, we do not observe the uplift phenomenons at the edges of the scratch track. It could be concluded that the content of soft material, namely copper, was high. The increased load may only lead to severe plastic deformation of the coating. In Fig.4(c), there was clear uplift accompanied with a large continuous flaking at the edges. At the end of the scratch track (Fig.4(c)), there was small amount crumbling coating.

So far, we can see that the coating adhesion failure of the coating-substrate system appeared in the three samples. The coating adhesion failure indicated that the coating or the coating and the substrate system crumbled in the form of fragmental caving inside the coating layer or the substrate layer located under the tip. However, the interface between the coating and the substrate did not failure, which means that the strong adhesion force results in coating adhesion failure between the coatings and substrates.

3.3 Tribological properties

The friction coefficient of the coating deposited on the Ti6Al4V substrate was measured against the alumina balls. Fig.5 shows the friction curves of the coatings and the substrates. In Fig.5, we can observe that the friction coefficients of the coatings and the substrate were different. At the beginning, the value of friction coefficient of the substrate was small, then it rose and fluctuated within a certain range. It should be noted that the contact area between the coating and the alumina ball was small, and the contact point was smooth at the beginning of the friction. Therefore, the value of the friction resistance was small. With the friction test running, the actual contact area between the coating and the alumina ball became large and rough, so was the wear of the contact surface. Finally, the friction coefficient increased and reached a steady state (Fig.5(c)).

In addition, the friction coefficient of the coatings was less than 0.45 of the substrate (Fig.5).

For sample C1, its friction coefficient was the least, the average friction coefficient was 0.19 in the stable phase, which was less than 1/2 time of the substrate. This phenomenon could be explained that there was hard TiN in sample C1, and the TiN can increase the abrasion resistance of the coating.The high content of Ti and the existence of Cu in the grinding way could increase the anti-friction ability of the substrate. Therefore, the friction coefficient decreases.

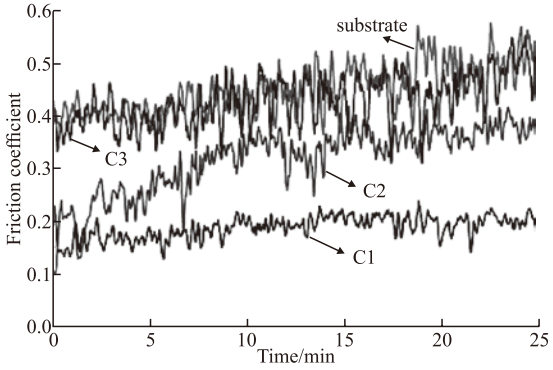

Fig.5 Friction coefficients of substrate and samples

The Cu content in sample C2 was more than that in sample C1, and stayed stable in the whole coating. Cu is a kind of soft material and can play a role of lubrication during the wear test. Therefore, the value of the friction coefficient decreases, as shown in Fig.5.

The friction coefficient measured using sample C3 is about 0.43, which is only slightly smaller than that of the substrate (Fig.5). It was indicated that the content of Cu in the coating was fairly high (up to 41 wt%). The large plastic deformation easily occurred in the process of the wearing and shearing on the surface of the coatings when the coating was under the external force due to the high content of copper. There was small deformation occurred in the TiN layer under the force of the ball. The coating contained less TiN. Due to the uncoordinated deformation, the stress concentration happened between the coatings and the substrate, which easily led to the rupturing of the coatings. The rupturing coatings were maxed in the grinding way, resulting in constantly scratch with the coating, so the friction coefficient of sample C3 increased.

Fig.5 shows the fluctuation of the friction coefficient. Compared with sample C1, the changes of the value of friction coefficient of sample C2 and C3 were remarkable in the beginning of the tribological curves. The main reason was the increased roughness of the coatings. The values of the friction coefficient of sample C2 and C3 are stable (Fig.5).

The wear tracks of the coatings and the Ti6Al4V are displayed in Fig.6. We can observe that there was no remarkable difference between the wear tracks of the substrate and the coatings. The width of the wear track was in the range of 723-784 μm, and the depth was about 10 μm. The width of sample C3 was the largest, and its properties of wear resistance became worse lightly.

The wear volumes of samples C1, C2 and C3 are listed in Table 2. The wear rates which were corresponding to Table 2 are shown in Fig.7. The difference between the wear rate of the samples and the substrate was small (Fig.7). We observe that the wear

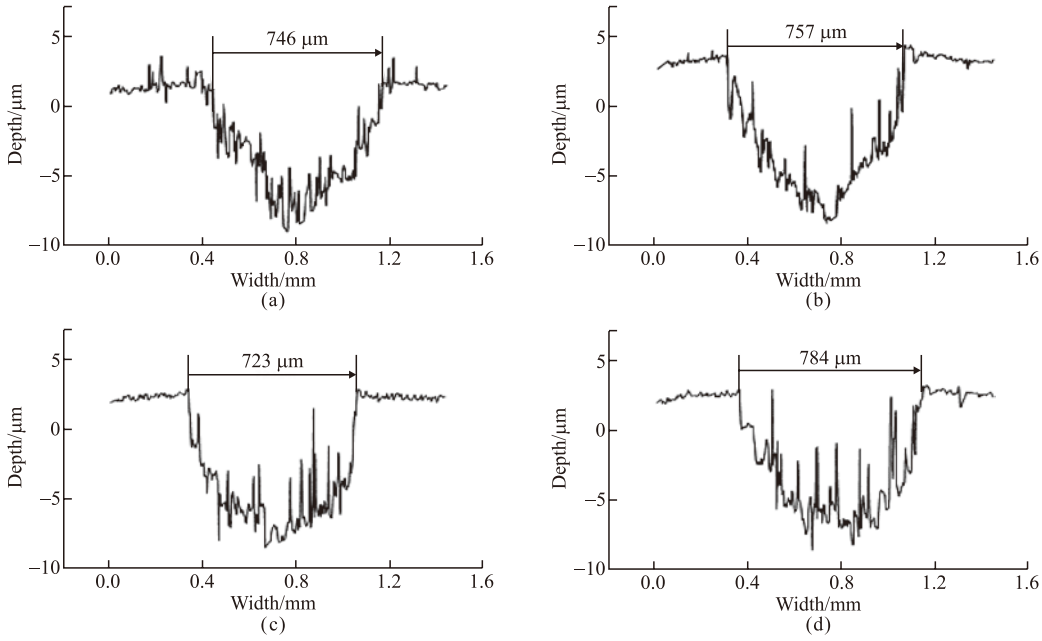

Fig.6 Cross-section profile of grinding track of the substrate and samples: (a) substrate; (b) C1; (c) C2; (d) C3

volume and wear rate of C1 were the greatest, as shown in Table 2 and Fig.5. In sample C1, the thickness of the N layer was only 0.7 μm, and the rest were large soft metal Ti and little amount of soft metal Cu. During the course of dry friction, the low content of soft metal can play a role of solid lubrication. That was the reason for that the uneven surface of alumina balls could be filled with soft metal in the wear test. The existence of the soft metal reduced the friction coefficient of the surface and improved the wear resistance[25]. However, the hardness would be reduced seriously. Since the high content of soft metal had negative effect on the wear resistance, the coating of sample C3 also had a high wear ratio because of the high Cu content. So in order to obtain better wear-resisting coatings, we should control and optimize the content of Ti, Cu and N. In this experimental study, sample C2 reached the expected wear resistance.

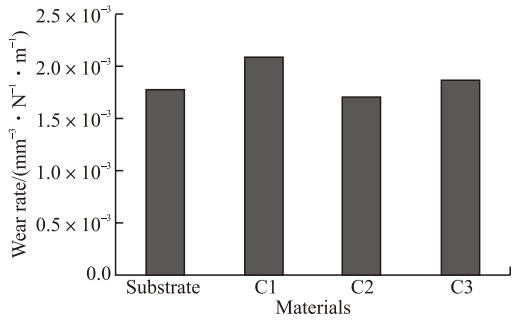

Fig. 7 Wear rate of substrate and samples

Table 2 Wear volume-loss of substrate and samples

Item	Substrate	C1	C1	C3
Wear volume/(10^{-2}·mm^{-3})	2.67	3.12	2.56	2.56

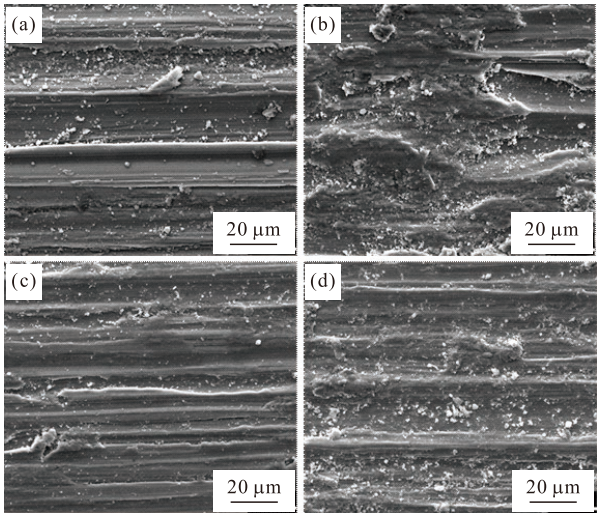

Fig.8 Wear morphologies of substrate and samples: (a) substrate; (b) C1; (c) C2; (d) C3

Fig.8 shows the surface wear morphologies of the substrate and samples C1, C2 and C3 after wear test. The load on each sample and test time were 1 N and 1 500 s respectively. The results (Fig.8) were magnified by 2 000 times . From the wear morphologies, we can observe that the coatings of the samples were not worn out. It could be explained that the light substrates were not shown inside wear morphologies. In Fig.8(a), parallel friction zone can be found and there were a lot of abrasive dusts in the friction zone. From the remarkable furrows and groove marks, we could concluded that the hardness of the substrate was less than the alumina grinding balls. So the hard particles on the grinding balls had a cutting effect on the Ti6Al4V substrate, and some chips fell off irregularly due to the plough. The furrows were formed by the cutting action of abrasive particles. The width of some furrows is large (Fig.8(a)), which indicated that the stress distribution was nonuniform. So the main wear mechanism of the substrate was abrasive wear and cutting wear.

The wear morphologies of sample C1 are shown in Fig.8(b) and it can be seen that sample C1 is worn seriously and has a large area of scratches. The furrows, a lot of abrasive dusts and abrasive particles could be found, and the accumulation and adhesion of the abrasive dusts came out. Under the action of the normal load, the micro-convex on the surface of the coating would have plastic deformations when the pressure of the tip exceeded the yield strength of the C1 coating. The surface coating ruptured when the friction pair slided relatively. The contact point of the cold welding would be formed in the contact area. In the subsequent sliding, the adhesion point was cut down and separated, the abrasive dust fell from the surface and formed a new adhesion point in the other area. In the process of the continual cutting, the new adhesion points were formed. In addition, wear occurred through metal-to-metal contact. The cycle process can be described as follows: contact-plastic deformation-surface coating rupture-adhesion(cold welding)-cutting down-falling off-adhesion again. So the main wear mechanism was adhesive wear and abrasive wear.

There are some abrasive particles in Fig.8(c), the depth of the wear crack was shallow and the width was uniform which means that the stress distribution of the friction contact area was uniform. The plastic deformation happened in the wear process, the soft material that adhered to the wear track had a large deformation and played a lubricant role, which led the flatness to increase. Combined with the wear rate in the Fig.7, the wear resistance of sample C2 is the best of

all and has higher wear resistance than the substrate. Fig.8(d) shows the wear morphologies of sample C3. A large amount of the abrasive dusts and abrasive particles can be found while the wear morphologies were uniform. This was highly related to the roughness of sample C3. The micro-convex bodies on surface would increase with the growing of the roughness. A large number of the abrasive dusts and abrasive particles were generated under the cutting action of the friction pair.

4 Conclusions

Ti/Cu/N coatings were deposited on the Ti6Al4V substrates by DCMS. With an increase of the Cu contents in the coatings, the number of large particles increased by FESEM. Through the scratch test, the Ti/Cu/N coatings showed an appreciable adhesion force. Tribological test indicated that there was a significant improvement in the wear resistance of the coatings by optimizing and controlling the relative content of Ti, Cu, N elements especially the 10.98 at% contents of the copper on the titanium alloy surface. Therefore, we could conclude that the DCMS technique may be better suited for depositing Ti/Cu/N composite coatings for various applications.

Acknowledgment

The first author gratefully acknowledged the helpful discussions with the research group and colleagues in the School of Mechanical Engineering at Taiyuan University of Technology.

References

[1] Geetha M, Singh A K, Asokamani R, *et al*. Ti Based Biomaterials, the Ultimate Choice for Orthopaedic Implants - A Review[J]. *Prog. Mater. Sci.*, 2009,54 (3): 397-425

[2] Grupp T M, Meisel H J, Cotton J A, *et al*. Alternative Bearing Materials for Intervertebral Disc Arthroplasty[J]. *Biomaterials*, 2010, 31: 523-531

[3] Wang S, Liao Z H, Liu Y H, *et al*. Different Tribological Behaviors of Titanium Alloys Modified by Thermaloxidation and Spraying Diamond Like Carbon[J]. *Surf. Coat. Technol.*, 2014, 252: 64-73

[4] Thorwarth G, Hammerl C, Kuhn M, *et al*. Investigation of DLC Synthesized by Plasma Immersion Ion Implantation and Deposition[J]. *Surf. Coat. Technol.*, 2005, 193: 206-212

[5] Krishna D S R, Brama Y L, Sun Y. Thick Rutile Layer on Titanium for Tribological Applications[J]. *Tribol. Int.*, 2007, 40: 329-334

[6] Li J, Sun M, Ma X. Structural Characterization of Titanium Oxide Layers Prepared by Plasma Based ion Implantation with Oxygen on Ti6A14V Alloy[J]. *Appl. Surf. Sci.*, 2006, 252 (20): 7 503-7 508

[7] Sun R L, Lei Y W, Niu W. Laser Clad TiC Reinforced NiCrBSi Composite Coatings on Ti-6Al-4V Alloy Using a CW CO_2 Laser[J]. *Surf. Coat. Technol*., 2009, 203: 1 395-1 399

[8] Yoon J S, Myung H S, Han J G. A Study on the Synthesis and Microstructure of WC-TiN Superlattice Coating[J]. *Surf. Coat. Technol*., 2000, 131: 372

[9] Shi Y L, Peng H R, Xie Y, *et al*. Plasma CVD of Hard Coatings Ti(C-NO) Using Metallo-organic Compound $Ti(OC_3H_7)_4$[J]. *Surf. Coat. Technol.*, 2000, 132: 26

[10] Endler I, Hohn M, Herrmann M, *et al*. Aluminum-rich TiAlCN Coatings by Low Pressure CVD[J]. *Surf. Coat. Technol.*, 2010, 205: 1 307

[11] Behrens B A, Huskic A. Verschleißreduzierung an Matrizen für das Präzisionsschmieden von Zahnrädern durch Mehrlagenhartstoffbeschichtung (TiN-TiCN-TiC)[J]. *Materialwiss. Werkst.*, 2005, 36: 218

[12] Agudelo L C, Ospina R, Castillo H A, *et al*. Synthesis of Ti/TiN/TiCN Coatings Grown in Graded Form by Sputtering DC[J]. *Phys. Scr.*, 2008, 131: 014 006

[13] Wang S, Liao Z H, Liu Y H, *et al*. Recent Development on Surface Modification of Artificial Disc Material for Wear Resistance[J]. *J. Funct. Mater.*, 2013, 5 (44): 609-613

[14] Zheng J H, Hao J Y, Liu X Q, *et al*. A Thick TiN/TiCN Multilayer Film by DC Magnetron Sputtering[J]. *Surf. Coat. Technol.*, 2012, 209: 110-116

[15] Wang X Q, Zhao Y H, Yu B H, *et al*. Deposition, Structure and Hardness of Ti–Cu–N Hard Films Prepared by Pulse Biased Arc Ion Plating[J]. *Vacuum.*, 2011, 86: 415-421

[16] Zhang L, Ma G J, Lin G Q, *et al*. Nuclear Instruments and Methods in Physics Research Section B: Beam Interactions with Materials and Atoms[J]. *Nuclear Instruments and Methods in Physics Research B*, 2014, 320: 17-21

[17] Zhao Y H, Wang X Q, Xiao J Q, *et al*. Ti-Cu-N Hard Nanocomposite Films Prepared by Pulse Biased Arc Ion Plating[J]. *Appl. Surf. Sci.*, 2011, 258: 370-376

[18] Myung H S, Lee H M, Shaginyan L R, *et al*. Microstructure and Mechanical Properties of Cu Doped TiN Superhard Nanocomposite Coatings[J]. *Surf. Coat. Technol.*, 2003, 163-164 : 591-596

[19] Wang H F, Shu X F, Guo M Q, *et al*. Structural, Tribological and Antibacterial Activities of Ti-Cu-N Hard Coatings Prepared by Plasma Surface Alloying Technique[J]. *Surf. Coat. Technol.*, 2013, 235: 235-240

[20] Bao M D, Yu L, Xu X B, *et al*. Microstructure and Wear Behaviour of Silicon Doped Cr-N Nanocomposite Coatings[J]. *Thin Solid Films*, 2009, 517: 4 938

[21] Hu M, Gao X M, Weng L J, *et al*. The Microstructure and Improved Mechanical Properties of Ag/Cu Nanoscaled Multilayer Films Deposited by Magnetron Sputtering[J]. *Appl. Surf. Sci.*, 2014, 313: 563-568

[22] Grant D M, Lo W J, Parker K G, *et al*. Biocompatible and Mechanical Properties of Low Temperature Deposited Quaternary (Ti, Al, V) N Coatings on Ti6Al4V Titanium Alloy Substrates[J]. *J. Mater Sci: Mater. Med.*, 1996, 7: 579-584

[23] Thornton J A. High Rate Thick Film Growth[J]. *Annual Review of Materials Science*, 1977, 7(1): 239-260

[25] Haseeb A, Celis J P, Roos J R. Fretting Wear of Metallic Multilayer Films[J]. *Thin Solid Films*, 2003, 444(1): 199-207